International Journal of Pharmaceutics: X 3 (2021) 100099

Contents lists available at ScienceDirect

International Journal of Pharmaceutics: X

journal homepage: www.sciencedirect.com/journal/international-journal-of-pharmaceutics-x

Downstream processing of spray-dried ASD with hypromellose acetate succinate – Roller compaction and subsequent compression into high ASD load tablets

Andreas Sauer [a,*], Shogo Warashina [b], Saurabh M Mishra [c], Ilja Lesser [a], Katja Kirchhöfer [a]

[a] SE Tylose GmbH & Co. KG, Kasteler Str. 45, 65203 Wiesbaden, Germany
[b] Shin-Etsu Chemical Co. Ltd, 28-1 Nishifukushima, Kubiki-ku, Joetsu-shi, Niigata, Japan
[c] SE Tylose USA Inc, Pharmaceutical Application Laboratory, Totowa, NJ 07512, USA

ARTICLE INFO

Keywords:
Hypromellose acetate succinate
Spray drying
Dry granulation
Downstream processing
Amorphous solid dispersion
Low-substituted hydroxypropyl cellulose

ABSTRACT

Despite wide commercial application of hypromellose acetate succinate (HPMCAS) in spray-dried amorphous solid dispersion (ASD) drug products, little information is available in the references on downstream processing of spray-dried dispersions with HPMCAS. Poor flow and high dilution factor are a challenge in formulating spray-dried ASDs into tablets, leaving little space for other excipients facilitating binding and disintegration. Direct compression is not possible due to the poor powder flow of spray-dried ASDs. Moisture has to be avoided due to the plasticizing properties of water on the ASD, resulting in reduced stability of the amorphous state. Thus, dry granulation by roller compaction and subsequent tablet compression is the preferred downstream process. We report the investigation of downstream processing by roller compaction and tablet compression of a high load formulation with 75% of spray-dried amorphous solid dispersion (Nifedipine:HPMCAS 1:2). A head to head comparison of microcrystalline cellulose/croscarmellose (MCC/cl-NaCMC) as binder/disintegrant vs. MCC and low-substituted hydroxypropyl cellulose (L-HPC) as excipient for binding and disintegration showed improved re-workability of the formulation with MCC/L-HPC after roller compaction. Upon transfer to the rotary press, a 45% higher tensile strength of tablets is observed after dry granulation with MCC/L-HPC.

1. Introduction

Amorphous solid dispersion (ASD) is one important strategy to formulate poorly soluble BCS class II drugs into commercial drug products. To overcome low aqueous solubility, the API is processed with a carrier polymer to transfer the crystalline API into a molecularly dispersed amorphous state with increased solubility (Baghel et al., 2016; Schittny et al., 2020). Different polymers and technologies are established to yield amorphous solid dispersion drug products. Commercialized solid dispersions rely on cellulosic polymers (e.g. Hypromellose acetate succinate HPMCAS, Hypromellose HPMC) or on synthetic polymers (e.g. PVP/VA copolymer, PVP or PEG) as carrier polymer. Technologies to produce solid dispersion includes spray drying, hot melt extrusion, co-precipitation, fluid bed granulation, and recently the Kinetisol process and others have been reported (Friesen et al., 2008; Hughey et al., 2015; Mendonsa et al., 2020; Sandhu et al., 2014). However commercial products mostly rely on spray drying and hot melt extrusion technology (Matić et al., 2020; Solanki et al., 2019; Zhang et al., 2018). Spray drying is one of the preferred technology for formulating amorphous solid dispersion with HPMCAS. Examples of commercialized drug products prepared by spray drying with HPMCAS are collated in Table 1. Commercial ASD products feature usually large tablet size (6 out of 7 of Table 1) due to the dilution effect of the ASD formulation (Dailymed, 2021). To stabilize amorphous solid dispersion over shelf life, e.g. prevent API crystallization, the ratio between drug and carrier polymer is typically in the range of 1:9 to 4:6. (Henriques et al., 2020; Mudie et al., 2020; Schittny et al., 2020).

After spray drying the API with the carrier polymer, the ASD shows low bulk density and poor powder flow, preventing direct compression into tablets on a rotary tablet press. Roller compaction dry granulation is usually applied as downstream process to improve the particle size and powder flow of spray-dried powders (Démuth et al., 2015; Henriques et al., 2016). The ASD is roller compacted with a filler and a disintegrant to provide granules, which are subsequently compressed into tablets or

* Corresponding author.
E-mail address: andreas.sauer@setylose.com (A. Sauer).

https://doi.org/10.1016/j.ijpx.2021.100099
Received 23 July 2021; Received in revised form 30 September 2021; Accepted 1 October 2021
Available online 14 October 2021

Table 1
Commercialized spray-dried ASD products with HPMCAS as carrier polymer. A complete list of inactive ingredients is given in the supporting information (Baghel et al., 2016; CHMP, 2018; Solanki et al., 2019).

Name	Drug	API dose (mg)	Tablet size and shape [a]	Contains 'MCC/cl-NaCMC
Incivek (discontinued)	Telaprevir	375	20 mm, Oval	Yes
Kalydeco	Ivacaftor	150	5 mm, Oval	Yes
Orkambi	Lumacaftor/Ivacaftor	200, 125	14 mm, Oval	Yes
Symdeko Morning Dose	Tezacaftor/Ivacaftor	100 + 150	16 mm, Capsule	Yes
Symdeko Evening Dose	Ivacaftor	150	17 mm, Capsule	Yes
Delstrigo	Doravirine (+Lamivudine, Tenofovir disoproxil fumarate)	100, 300, 300	22 mm, Oval	Yes
Pifeltro	Doravirine	100	19 mm, Oval	Yes

[a] Size information for oval or capsule shaped tablets describe the long axis.

Table 2
Formulations studied.

	F1 MCC/cl-NaCMC (*w*/w) (%)	F2 MCC/L-HPC (w/w) (%)
Nifedipine:HPMCAS SDD	75.0	75.0
L-HPC NBD-021	–	15.0
MCC-101	20.5	8.5
cl-NaCMC	3.0	–
Silicon dioxide	0.5	0.5
Magnesium stearate[a]	1.0	1.0

[a] 0.5% Magnesium stearate was added in the RC step and 0.5% prior to tablet compression.

filled into capsules. Typical excipients in dry granulation include microcrystalline cellulose (MCC), lactose, or calcium phosphate as filler and a disintegrant like croscarmellose (cl-NaCMC) or crospovidone. For high dose drug products with poorly compressible APIs, dry binders are used to increase the compactibility the powder blend. (Arndt and Kleinebudde, 2018; Herting et al., 2007; Mangal et al., 2016; Sun and Kleinebudde, 2016). Interestingly, in the case of the commercial ASD examples (Table 1) no dry binder is used and all examples are formulated with MCC/croscarmellose as binder and disintegrant. Using roller compaction dry granulation, loss of tabletability is encountered due to double compression of the formulation first in the roller compactor, and then in the tablet press. This behavior is described as work- or granule hardening (Herting and Kleinebudde, 2008; Sun and Himmelspach, 2006; Sun and Kleinebudde, 2016). More specific, a report on dry granulation of MCC revealed that increasing specific compaction forces in the roller compactor for different MCC grades resulted in a reduced tensile strength after tablet compression due to work hardening. (Herting and Kleinebudde, 2008). Low-substituted hydroxypropyl cellulose (L-HPC) is an excipient used as disintegrant and binder due to its swelling and compressibility (Alvarez-Lorenzo et al., 2000; ElShaer et al., 2018; Onuki et al., 2018). L-HPC is available in different particle sizes and substitutions. A reduction in particle size yields tablets with higher tensile strength, while increasing the hydroxypropoxy substitution results in an increase in disintegration time. (Alvarez-Lorenzo et al., 2000; ElShaer et al., 2018). Recently, L-HPC was included in a systematic study with 81 excipients in roller compaction. L-HPC was, among others, categorized as category 1 material providing ribbon tensile strength >1 MPa with $0.6 \leq SF \leq 0.8$ at low hydraulic pressure (30–70 bar) (Yu et al., 2019). However, there is no report on the application of L-HPC in spray-dried dispersion downstream processing. Despite the popularity of HPMCAS in commercial formulation, there are few references on dry granulation of spray-dried ASDs with HPMCAS as carrier polymer. Reports however are available on direct compression of spray dried dispersions (SDDs) with HPMCAS in single punch equipment to study compactibility of spray-dried powders (Honick et al., 2020; Iyer et al., 2013; Roberts et al., 2011). These however do not resemble the industry practice of tablet compression after roller compaction. The authors suggest that the limited reports of RC of spray-dried material are attributed to low productivity of lab-scale spray drying equipment, delivering insufficient amounts of SDD for roller compaction experiments. Thompson et al., 2010 reported 2010 on the compactibility of spray-dried HPMCAS:SLS blends in dry granulation with MCC 102. They report the reduction of ribbon tensile strength and tablet tensile strength in comparison to spray-dried HPMCAS without SLS (Thompson et al., 2010). Mudie et al. reported on roller compaction of spray-dried erlotinib:Eudragit L100 (65:35) using HPMCAS AS-HF externally in the roller compaction step to prepare novel high drug load ASD tablets after granules compression with MCC 101, lactose and croscarmellose. In this study, HPMCAS was found to increase the parachute effect of the dissolution profile as precipitation inhibitor after dissolution, and is not utilized as ASD carrier. In comparison with a SDD with erlotinib: HPMCAS (35:65) which was slugged prior to tablet compression, the release in high gastric pH = 6 was slower and a lower c_{max} was observed. (Mudie et al., 2020). A recent study from Henriques et al. describes spray drying and roller compaction of a non-disclosed API with PVP-VA (20:80). Roller compaction was carried out with MCC 102 as filler, crospovidone as disintegrant, and magnesium stearate as lubricant. Variation of roller pressure and sieve mesh aperture showed larger impact on the granules properties like size, powder flow, and tabletability with additional impact of the gap size. They conclude that for spray-dried powders, mild roller compaction conditions are sufficient to enable a robust downstream process. (Henriques et al., 2020). The aim of this study is the investigation of roller compaction downstream processing and tablet compression of a formulation with a high load of spray-dried ASD using HPMCAS as carrier polymer. Nifedipine was selected as model API based on previous reports of nifedipine-HPMCAS ASDs (Sarabu et al., 2020; Tanno et al., 2004). MCC/cl-NaCMC or MCC/L-HPC were selected as filler/binder and disintegrating excipients in the formulation.

2. Materials and methods

A spray-dried solid dispersion of Nifedipine and HPMCAS (Shin-Etsu AQOAT® AS-MG), 1:2 ratio, and low-substituted hydroxypropyl cellulose (L-HPC NBD-021) was provided by Shin-Etsu Chemical Co. Ltd. (Japan). Microcrystalline cellulose (MCC, Pharmacel 101) and croscarmellose sodium (cl-NaCMC, Solutab A) were sourced from DFE (Netherlands) and Roquette (France) respectively. Silicon dioxide (Aerosil® 200 Pharma) was sourced from Evonik Industries AG (Germany) and magnesium stearate from Applichem (Germany). All materials were used as received after being stored at ambient condition for minimum two weeks. The powder properties of the Nifedipine:HPMCAS SDD are collated in table SI2 in the supporting information. Two formulation blends were prepared in a plastic bag (Table 2). Formulation 1 (F1) with high amount of solid dispersion was prepared with MCC as binder/filler and an industry typical amount of croscarmellose as disintegrant (Zhao and Augsburger, 2006), similar to the inactive ingredients in commercialized ASDs (Table 1). Formulation 2 was developed with L-HPC replacing part of MCC and all of croscarmellose. A preliminary study revealed that 15% of L-HPC gave a good balance of tablet hardness and low disintegration time (Figs. SI2 and SI3 in the supporting information).

Table 3
Particle size analysis of powders and granules by laser diffraction.

Run	D_{10} (μm)	D_{50} (μm)	D_{90} (μm)
F1 MCC/cl-NaCMC blend	6.95	37.02	95.95
F1 MCC/cl-NaCMC 5 kN/cm	10.01	51.14	702.64
F2 MCC/L-HPC blend	6.93	35.63	94.37
F2 MCC/L-HPC 5 kN/cm	10.17	47.41	567.56
F2 MCC/L-HPC 10 kN/cm	19.14	394.3	1068.3

2.1. Roller compaction

Roller compaction was carried out on an Alexanderwerk WP-120 (Alexanderwerk AG, Germany) with 25 mm knurled rollers at specific compaction forces (SCF) of 5 kN/cm (formulation 1 and 2) and 10 kN/cm (for formulation 2). Compaction was carried out at constant roller speed of 3.4 rpm, gap size of 2 mm, using sieve coarse and fine of 2.5 mm, and 1.25 mm respectively, The sieve velocity was 50 rpm in all roller compaction processes.

2.2. Evaluation of powder and granules properties

Bulk density, tapped density, and the angle of repose were analyzed according to the USP guidelines. The hausner ratio was calculated (tapped density/bulk density). Loss on drying was analyzed using a Kern DBS 60–3 moisture analyzer (KERN & SOHN GmbH). Particle size was determined using a laser diffraction HELOS & RODOS (Sympatec GmbH, Germany) with a dispersion pressure of 200 kPa. True density of powder and granules was analyzed at 20 °C using a Pycnomatic ATC EVO helium pycnometer (Thermo Fisher Scientific, USA). SEM micrographs were prepared on a JSM-IT100 scanning electron microscopy (JEOL, Japan).

2.3. Tablet compression

Single punch tablet compression was carried out on a Gamlen D-Series (Gamlen Tableting Ltd., UK) compaction analyzer. 50 mg of powder was weighted and transferred into the 5 mm punch and die set. Tablets were compressed at a dwell time of 120 ms and pressures of 25–225 MPa ($n = 3$). Rotary press compaction studies were carried out a Romaco Kilian Pressima (Romaco Kilian GmbH, Germany) rotary tablet press (200 mg, 8 mm, round, flat tablets) at a dwell time of 96 ms (10 rpm) at 100–200 MPa compression pressure.

2.4. Tablet analysis

Tablets were stored at ambient condition for 24 h prior to analysis. Tablet hardness, thickness and diameter, tablet disintegration, tablet friability, and tablet dissolution were tested on an Erweka TBH225 ($n = 3$ for single punch compaction, $n = 10$ rotary press), Erweka ZT-322 ($n = 6$), Erweka TA120 (6.5 g of tablets, 100 rotations at 25 rpm), and on a Erweka DT720 dissolution tester equipped with UV analysis (USP apparatus 2, 50 rpm, 900 mL phosphate buffer pH = 6.8, λ = 238 nm, 0.055 mg/mL = 100% dissolved, $n = 3$).

2.5. Compressibility and compactibility analysis

Compaction analysis of tablets prepared on the single punch press was performed using the modified Heckel equation (Eq. (1)) to yield the compressibility parameter C and the percolation threshold ρ_c after fitting to ascertain compressibility. Details of the modified Heckel equation are described elsewhere (Kuentz and Leuenberger, 1999). Out-of-die data was used for compaction analysis calculations.

$$\sigma_c = \frac{1}{C}\left[\rho_c - \rho_r - (1-\rho_c)ln\left(\frac{1-\rho_r}{1-\rho_c}\right)\right] \quad (1)$$

σ_c = compaction pressure; C = compressibility parameter; ρ_r = solid fraction; ρ_c = percolation threshold.

The percolation model was used to yield compactibility (or tensile strength at zero porosity) σ_0 and the percolation threshold ρ_r to assess compactibility (Eq. (2)). The critical exponent q was chosen with 2.7 as reported before (Mishra and Rohera, 2019).

$$\sigma_t = \sigma_0\left(\frac{\rho_r - \rho_c}{1-\rho_c}\right)^q \quad (2)$$

σ_t = tensile strength; σ_0 = tensile strength at zero porosity; ρ_r = solid

Table 4
Powder analysis of blended powders and granules.

Run	Bulk density (g/cm³)	Tapped density in (g/cm³)	Hausner Ratio [−]	Angle of repose (°)	LOD (%)
F1 MCC/cl-NaCMC blend	0.344	0.502	1.46	Nd[a]	1.87
F1 MCC/cl-NaCMC 5 kN/cm	0.566	0.682	1.20	38.79	2.03
F2 MCC/L-HPC blend	0.345	0.500	1.45	Nd[a]	1.79
F2 MCC/L-HPC 5 kN/cm	0.544	0.678	1.25	37.04	1.78
F2 MCC/L-HPC 10 kN/cm	0.600	0.769	1.28	38.02	1.82

[a] Not determined, no powder flow through the funnel observed.

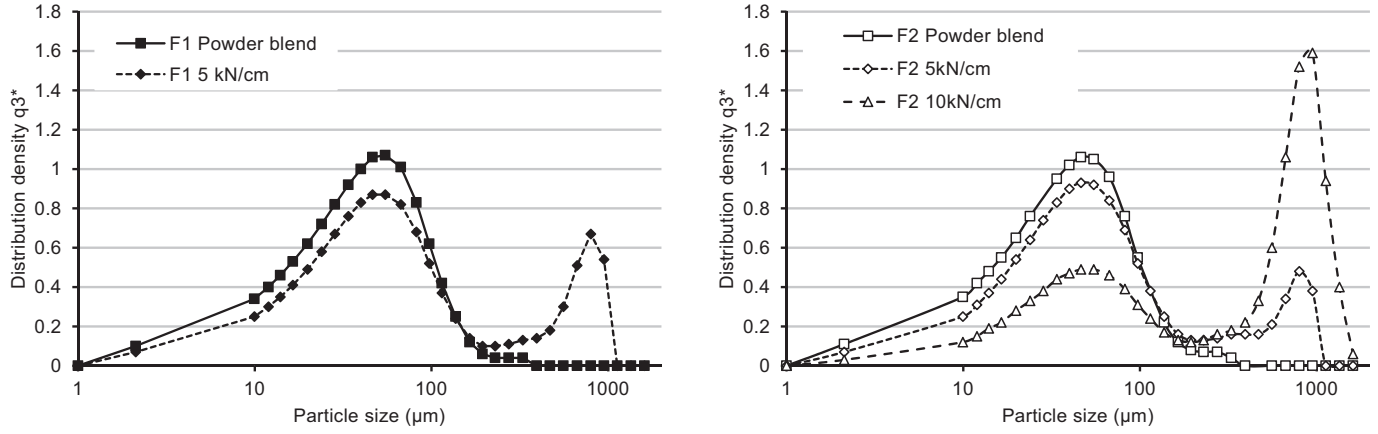

Fig. 1. Particle size distribution for F1 (left) and F2 (right) at different specific compression forces.

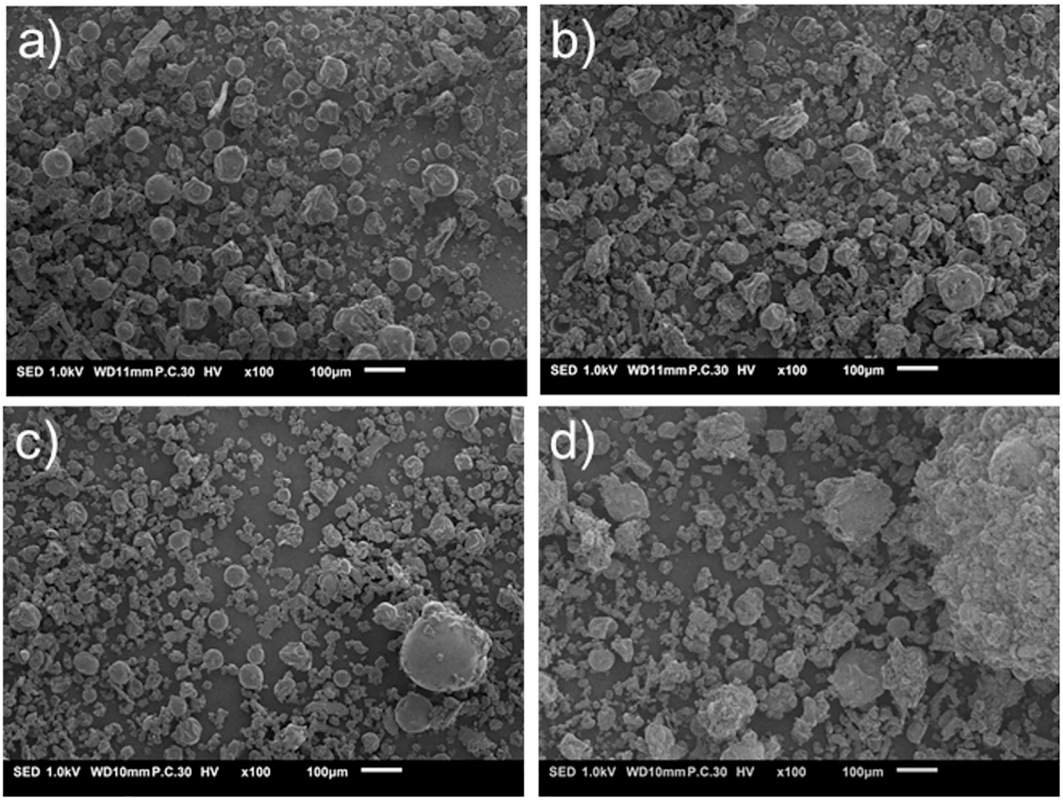

Fig. 2. SEM Micrographs of F1 (a, b) and F2 (c, d) before granulation (left) and after granulation with 5 kN/cm (right).

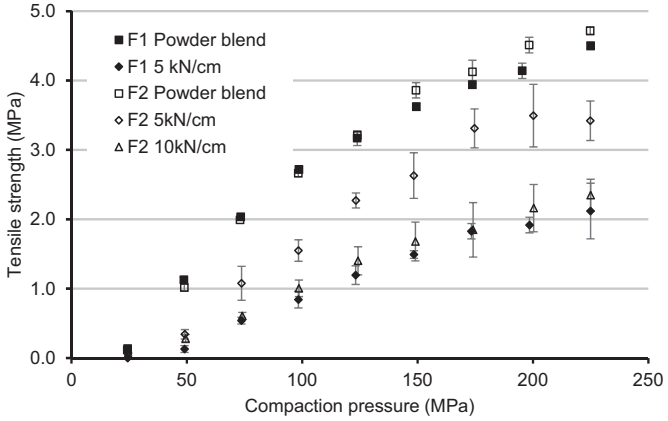

Fig. 3. Tabletability plot of compression pressure vs. tensile strength.

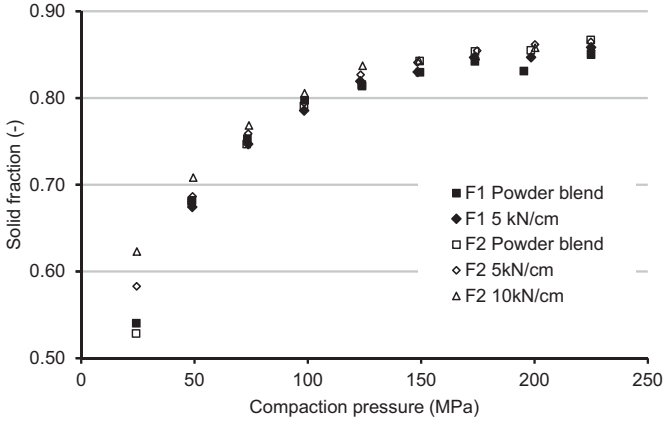

Fig. 4. Compressibility plot of compression pressure vs. solid fraction.

fraction; ρ_c = percolation threshold; q = critical exponent = 2.7.

3. Results and discussion

3.1. Roller compaction

Formulation 1 with MCC/cl-NaCMC and formulation 2 with MCC/L-HPC and 75% ASD content were subjected to roller compaction by lubricating with 0.5% magnesium stearate. Dry granulation proceeded smoothly and granules were collected. Both formulations showed a slight increase in medium particle size when granulating with 5 kN/cm and a similar D_{50} is obtained for F1 and F2 (Table 3). Bimodal particle size distributions were observed with both formulations (Fig. 1) where an increase in the coarse fraction was observed while most of the initial powder particles remain. Increasing the SCF to 10 kN/cm for formulation 2 further increased the coarse particle size fraction and an increase in D_{50} was observed. A bimodal particle size distribution is typical for roller compaction processes as the initial powder is recovered after milling of the ribbon or due to leakage of the powder through the roller seals (Henriques et al., 2020; Mangal et al., 2016). Additional trials with formulation 1 at 10 kN/cm SCF were not possible due to limited availability of the SDD. Analysis of bulk density showed a large increase in bulk density at 5 kN/cm specific compaction force on the roller compactor (Table 4). Further increase in SCF to 10 kN/cm resulted in a slight increase in bulk density. The Hausner ratio was reduced for both formulations compacted at 5 kN/cm in comparison to the uncompacted powder and free-flowing granules were obtained, whereas both powder blend could not flow from a funnel (see the video on flow difference of F2 uncompacted and compacted at 5 kN/cm: F2 Flow.mp4). This was confirmed by compacted formulations showing a low

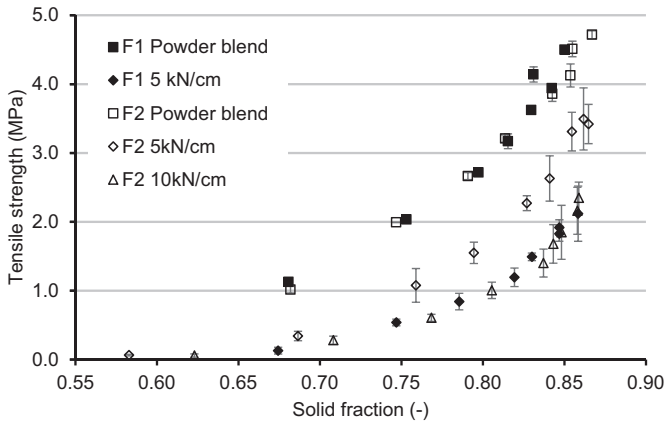

Fig. 5. Compactibility plot of solid fraction vs. tensile strength.

Table 5
Fit parameters for the modified Heckel equation.

Formulations	Compressibility parameters (1/C), (MPa)	Percolation threshold (ρ_c)	R^2
F1 Powder blend	990.10 ± 42.85	0.540 ± 0.070	0.9059
F1 5 kN/cm	740.74 ± 29.66	0.496 ± 0.058	0.9403
F2 Powder blend	558.65 ± 27.14	0.446 ± 0.063	0.9571
F2 5 kN/cm	628.93 ± 28.10	0.478 ± 0.060	0.9525
F2 10 kN/cm	869.56 ± 37.20	0.542 ± 0.0.064	0.9209

Table 6
Fit parameters for the percolation model.

Formulations	Compactibility σ_0, (MPa)	Percolation threshold (ρ_c)	R^2
F1 Powder blend	10.19 ± 0.45	0.451 ± 0.032	0.9815
F1 5 kN/cm	6.73 ± 0.49	0.598 ± 0.015	0.9889
F2 Powder blend	9.66 ± 0.33	0.439 ± 0.016	0.9953
F2 5 kN/cm	9.94 ± 0.53	0.579 ± 0.013	0.9936
F2 10 kN/cm	7.91 ± 1.04	0.632 ± 0.023	0.9737

angle of repose of granules. (Carr, 1965). Compacting formulation 2 at higher specific compaction force of 10 kN/cm did not result in further improvement of powder flow. Both formulations showed an increase in bulk density with a small increase in particle size at low SCF of 5 kN/cm. At low SCF, the compaction energy is hypothetically mostly absorbed by the hollow spherical ASD particles resulting in compressed ASD particles with increased bulk density, but only a slight increase in particle size. SEM micrographs confirmed the compressed appearance of ASD particles after granulation at 5 kN/cm (Fig. 2). When a higher SCF of 10 kN/cm was applied to formulation 2, an increase in particle size was observed, however bulk density increased only slightly in comparison to the same formulation granulated with a SCF of 5 kN/cm. At 10 kN/cm, the compaction energy is absorbed by the ASD particles and surplus energy was turned into particle size enlargement, leading to the observed increase in particle size.

3.2. Single punch compaction analysis

Powders and granules of F1 and F2 were compacted on a single punch compaction analyzer at different compression pressures (25–225 MPa). The moisture content of all blends before compaction was similar (LOD 1.8–2.0%). Figs. 3–5 show the compaction triangle diagrams tabletability, compressibility, and compactibility for all formulations and processing conditions (Tye et al., 2005).

The tabletability plot reveals that both non-granulated powder blends formulation F1 and F2 showed a similar compression profile. After roller compaction at SCF 5 kN/cm however the granules F1 or F2 showed a reduced tablet tensile strength after tablet compression. For F1 with MCC/cl-NaCMC, the reduction of tensile strength is higher (59% reduced TS at 150 MPa compression pressure) compared to formulation 2 featuring MCC/L-HPC (32% reduced TS at 150 MPa compression pressure). When increasing the specific compaction force from 5 kN/cm to 10 kN/cm a further decrease in tensile strength is observed. For tablets, a tensile strength of >1.7 MPa at SF < 0.85 is considered acceptable for further processing which was observed with granules prepared with SCF of 5 kN/cm granules for formulations F1 at 175 MPa compression pressure and for formulation F2 at 125 MPa (Leane et al., 2015; Pitt and Heasley, 2013).

The compressibility plot describes the reduction of volume (porosity) with application of pressure. Qualitative analysis reveals that the solid fraction of tablets increased with increasing compaction force on the roller compactor in the dry granulation step and in tablet compression (Fig. 4). Typical solid fractions for pharmaceutical tablets is 0.85 ± 0.05 (Hancock et al., 2003; Leane et al., 2015) which is reached at 100 MPa compression pressure on the tablet press. Formulation F2 processed at 10 kN/cm showed the highest solid fraction of tablets until 125 MPa compression pressure due to the high compression at the granulation step.

The modified Heckel equation describes the compression behavior of pharmaceutical powders (Kuentz and Leuenberger, 1999). Compression parameter 1/C and the percolation threshold ρ_c for the fit is given in Table 5 (Fig. SI4 in the supporting information). Comparing granules of F1 and F2 compressed at 5 kN/cm specific compaction force on the roller compactor, the lower 1/C value for formulation 2 with MCC/L-HPC indicates higher compressibility and plasticity. Increasing the roller

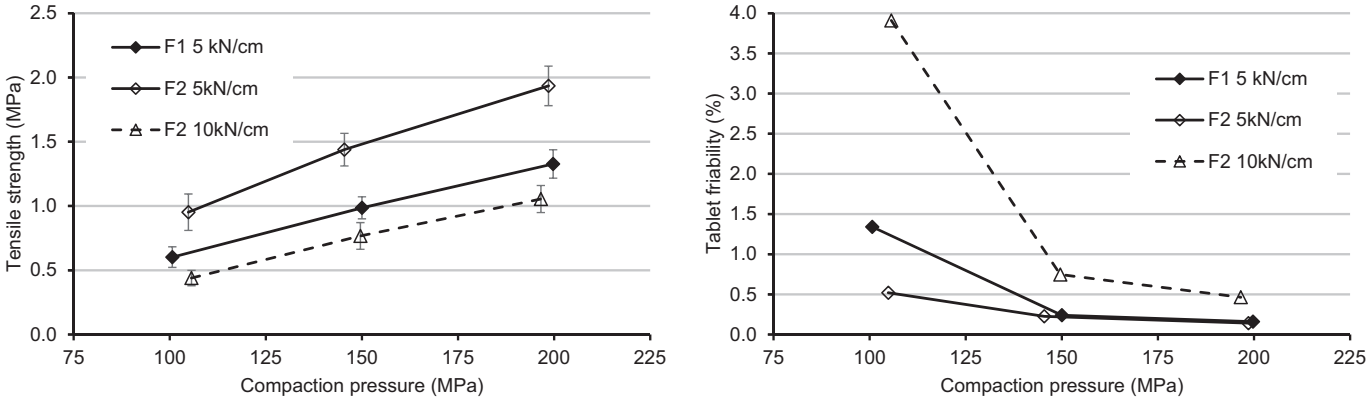

Fig. 6. Left: Tensile strength vs. compaction pressure. Right: Tablet friability vs. compaction pressure (lines added as guide to the eye).

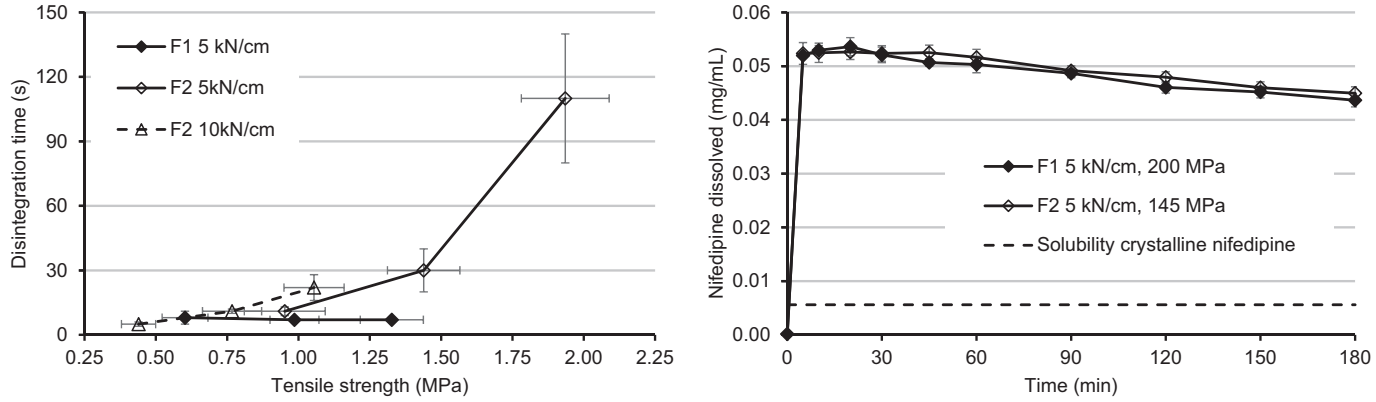

Fig. 7. Left: Tablet disintegration time vs. tensile strength. Right: Tablets dissolution profile (lines added as guide to the eye).

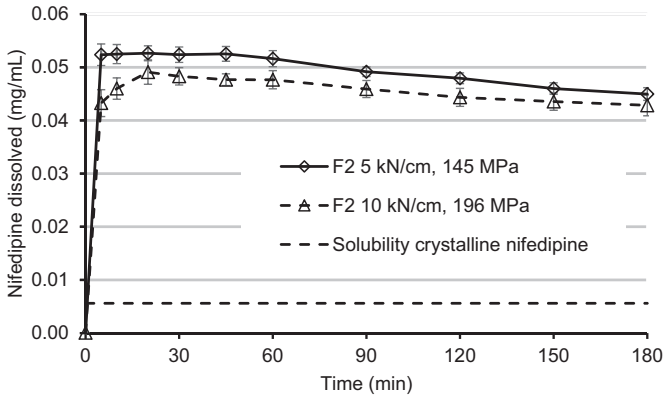

Fig. 8. Comparison of dissolution profiles for formulation 2 with different SCF during roller compaction (lines added as guide to the eye).

compaction force to 10 kN/cm, the compressibility is reduced as evident from the higher 1/C value, in agreement with work-hardening processes. Neat L-HPC NBD-021 shows a 1/C value of 99.52 ± 4.45 MPa with $\rho_c = 0.170 \pm 0.017$ (unpublished results).

The compactibility plot describes how reduction of volume (porosity) is transferred into tensile strength of the compact and is used to characterize powder compactibility independent of dwell time (Tye et al., 2005) Qualitative analysis reveals as expected highest compactibility for powder blends of F1 and F2 not processed on the roller compactor (Fig. 5). Formulation 1 processed at 5 kN/cm showed a reduced compactibility profile compared to Formulation 2 processed at 5 kN/cm. Formulation 2 processed at 10 kN/cm showed similar compactibility profile compared to formulation 1 at 5 kN/cm, which is attributed to the work- or granule hardening phenomenon (Herting and Kleinebudde, 2008; Sun and Himmelspach, 2006; Sun and Kleinebudde, 2016).

The percolation model is a mathematical description of how reduction of porosity (increase in solid fraction) is turned into tablet tensile strength (Mishra and Rohera, 2019). Fitting results are reported in Table 6 (Fig. SI5 in the supporting information). Similar to the Ryshkewitch-Duckworth model, a higher zero strength porosity describes a higher compactibility. A lower percolation threshold describes improved compactibility as the solid fraction required to obtain a stable compact is reduced. The compactibility of non-granulated powder blends F1 and F2, is highest, and their percolation threshold is lowest. When granulating F1 at 5 kN/cm, the compactibility was reduced in comparison to the uncompacted powder. Such loss in compactibility in comparison to the uncompacted blend was not observed when F2 was subjected to roller compaction at 5 kN/cm. The percolation threshold was increased for F1 and F2 when the powder was subjected roller compaction, meaning a higher solid fraction was required to yield a stable compact. When the roller compaction specific compaction force for F2 was increased from 5 kN/cm to 10 kN/cm, a reduction in compactibility, and a further increase in percolation threshold was observed.

3.3. Rotary press compaction

To ascertain the performance of F1 and F2 in industrial processes, granules of F1 (SCF of 5 kN/cm) and F2 (SCF of 5 kN/cm and 10 kN/cm) were compressed on the rotary press and tablets were evaluated. Powder blends of F1 and F2 could not be processed due to the poor powder flow. The tabletability plot (Fig. 6, left) confirmed the single punch compaction analysis result with formulation 2 showing a higher tablet tensile strength (+45% at 150 MPa) when granulated at same SCF than formulation 1 over a compression pressure range (100–200 MPa) typical in industrial processing. Comparing the tabletability plots from the single punch compaction analyzer (Fig. 3) and the rotary press (Fig. 6, left) reveals that throughout the study, at same compression pressure, the observed tablet tensile strength is lower on the rotary press compared to the compaction analyzer. However the order of reworkability on both equipment is the same with formulation 2 showing a higher tablet TS at same SCF than formulation 1 and the reduction of TS with increasing SCF as demonstrated in formulation 2. The authors attribute the difference in TS to a lower dwell time on the rotary press (96 ms vs. 120 ms on the compaction analyzer) which was reported before to influence tensile strength (Tye et al., 2005). This is supported by the lower solid fraction of tablets produced on the rotary press in comparison to the compaction analyzer (Fig. SI6 in the SI) and the comparative compactibility plot (Fig. SI7). Tablet friability was <0.25% at 150 MPa, and lower for tablets prepared with both formulations granulated at SCF of 5 kN/cm (Fig. 6, right). The increase in granulation SCF from 5 kN/cm to 10 kN/cm increased tablet friability and at 150 MPa compression pressure a friability of 0.75% was observed in case of formulation 2.

The disintegration time increased with increasing tensile strength in case of formulation 2 using MCC/L-HPC as binder and disintegrant (Fig. 7, left). At sufficient tensile strength (>1.75 MPa), the tablet disintegration time was up to two minutes for F2 granulated at SCF 5 kN/cm. Tablets with formulation 1 with MCC/cl-NaCMC showed low disintegration time (<7 s) independent of tensile strength of tablets, however maximum tensile strength achieved is 1.33 MPa at 200 MPa compression force, which is insufficient for industrial scale production (Pitt and Heasley, 2013). The dissolution profile of tablets with equivalent tensile strength prepared from F1 and F2, granulated with a SCF of 5 kN/cm were virtually identical despite the different disintegration time of tablets (Fig. 6, right). The solid dispersion of nifedipine and HPMCAS AS-MG (1:2) showed a > 10 fold solubility improvement with

stabilization of the supersaturation over 180 min. When increasing the SCF from 5 kN/cm to 10 kN/cm in formulation 2, a reduction of initial dissolution rate and maximum nifedipine dissolved was observed (Fig. 8). This is attributed to the larger particle size of granules in formulation F2 compacted at 10 kN/cm which limits dissolution rate.

4. Conclusion

A tablet formulation with high amount of spray-dried ASD (75% Nifedipine:HPMCAS 1:2 ratio) was developed using the widely commercially applied binder/disintegrant combination of MCC/croscarmellose, or MCC/L-HPC. Roller compaction of the ASDs reduced the compressibility and compactibility of the formulation while increasing bulk density and powder flow. At low specific compaction force of 5 kN/cm, the hollow spray-dried ASD particles were compressed and little granulation (particle size enlargement) was observed. At higher compaction force, the compaction energy was not fully absorbed by compression of the ASD particles and surplus energy was available for granulation (particle size enlargement) while further reducing compactibility. However, roller compaction at low SCF was sufficient to enable a robust tablet production process, showing that when designing roller compaction processes with spray-dried ASDs with HPMCAS, compression pressure should be selected carefully to avoid loss of tensile strength in downstream tablet compression. Tablets with high ASD load in the formulation, sufficient tensile strength for downstream coating or packaging, with rapid disintegration and quick dissolution are available by rational selection of the binder/disintegrant system.

Supplementary data to this article can be found online at https://doi.org/10.1016/j.ijpx.2021.100099.

Funding

This work was supported by SE Tylose GmbH & Co. KG.

Declaration of Competing Interest

Andreas Sauer reports financial support, article publishing charges, and equipment, drugs, or supplies were provided by SE Tylose GmbH & Co. KG. Andreas Sauer reports a relationship with SE Tylose GmbH & Co. KG that includes: employment. Co-Authors are employed by SE Tylose GmbH & Co. KG or other Shin-Etsu group companies.

Acknowledgement

We thank Hidetoshi Sakai from Shin-Etsu Chemical Co. Ltd. (Tokyo, Japan) for supplying the ASD of Nifedipine and HPMCAS and for its characterization.

References

Alvarez-Lorenzo, C., Gómez-Amoza, J.L., Martínez-Pacheco, R., Souto, C., Concheiro, A., 2000. Evaluation of low-substituted hydroxypropylcelluloses (L-HPCs) as filler-binders for direct compression. Int. J. Pharm. 197, 107–116. https://doi.org/10.1016/S0378-5173(99)00456-1.

Arndt, O.-R., Kleinebudde, P., 2018. Influence of binder properties on dry granules and tablets. Powder Technol. 337 https://doi.org/10.1016/j.powtec.2017.04.054.

Baghel, S., Cathcart, H., O'Reilly, N.J., 2016. Polymeric amorphous solid dispersions: a review of amorphization, crystallization, stabilization, solid-state characterization, and aqueous solubilization of biopharmaceutical classification system class II drugs. J. Pharm. Sci. https://doi.org/10.1016/j.xphs.2015.10.008.

Carr, R.L., 1965. Evaluating flow properties of solids. Chem. Eng. 72, 163–168.

CHMP, 2018. Assessment Report Pifeltro EMA/821709/2018. London.

Dailymed, 2021. WWW Document. URL. https://dailymed.nlm.nih.gov/dailymed/.

Démuth, B., Nagy, Z.K., Balogh, A., Vigh, T., Marosi, G., Verreck, G., Van Assche, I., Brewster, M.E., 2015. Downstream processing of polymer-based amorphous solid dispersions to generate tablet formulations. Int. J. Pharm. 486, 268–286. https://doi.org/10.1016/j.ijpharm.2015.03.053.

ElShaer, A., Al-khattawi, A., Mohammed, A.R., Warzecha, M., Lamprou, D.A., Hassanin, H., 2018. Understanding the compaction behaviour of low-substituted HPC: macro, micro, and nano-metric evaluations. Pharm. Dev. Technol. 23, 442–453. https://doi.org/10.1080/10837450.2017.1363775.

Friesen, D.T., Shanker, R., Crew, M., Smithey, D.T., Curatolo, W.J., Nightingale, J.A.S., 2008. Hydroxypropyl Methylcellulose Acetate Succinate-Based Spray-Dried Dispersions: An Overview, 5, pp. 1003–1019.

Hancock, B.C., Colvin, J., Mullarney, M.P., Zinchuk, A., 2003. The relative densities of pharmaceutical powders, blends, dry granulations, and immediate-release tablets. Pharm. Technol. 27, 64–80.

Henriques, J., Valente, P., Winters, C., 2016. Formulating amorphous solid dispersions: bridging particle engineering and formulation [WWW Document]. Am. Pharm. Rev. URL https://www.americanpharmaceuticalreview.com/Featured-Articles/331576-Formulating-Amorphous-Solid-Dispersions-Bridging-Particle-Engineering-and-Formulation/.

Henriques, J., Moreira, J., Doktorovová, S., 2020. QbD approach to downstream processing of spray-dried amorphous solid dispersions–a case study. Pharm. Dev. Technol. 26, 269–277. https://doi.org/10.1080/10837450.2020.1863985.

Herting, M.G., Kleinebudde, P., 2008. Studies on the reduction of tensile strength of tablets after roll compaction/dry granulation. Eur. J. Pharm. Biopharm. 70, 372–379. https://doi.org/10.1016/j.ejpb.2008.04.003.

Herting, M.G., Klose, K., Kleinebudde, P., 2007. Comparison of different dry binders for roll compaction/dry granulation. Pharm. Dev. Technol. 12, 525–532. https://doi.org/10.1080/10837450701557303.

Honick, M., Das, S., Hoag, S.W., Muller, F.X., Alayoubi, A., Feng, X., Zidan, A., Ashraf, M., Polli, J.E., 2020. The effects of spray drying, HPMCAS grade, and compression speed on the compaction properties of itraconazole-HPMCAS spray dried dispersions. Eur. J. Pharm. Sci. 155 https://doi.org/10.1016/j.ejps.2020.105556.

Hughey, J.R., Keen, J.M., Bennett, R.C., Obara, S., McGinity, J.W., 2015. The incorporation of low-substituted hydroxypropyl cellulose into solid dispersion systems. Drug Dev. Ind. Pharm. 41, 1294–1301. https://doi.org/10.3109/03639045.2014.947508.

Iyer, R., Hegde, S., Zhang, Y.E., Dinunzio, J., Singhal, D., Malick, A., Amidon, G., 2013. The impact of hot melt extrusion and spray drying on mechanical properties and tableting indices of materials used in pharmaceutical development. J. Pharm. Sci. 102, 3604–3613. https://doi.org/10.1002/jps.23661.

Kuentz, M., Leuenberger, H., 1999. Pressure susceptibility of polymer tablets as a critical property: a modified Heckel equation. J. Pharm. Sci. 88, 174–179. https://doi.org/10.1021/js980369a.

Leane, M., Pitt, K., Reynolds, G., 2015. A proposal for a drug product Manufacturing Classification System (MCS) for oral solid dosage forms. Pharm. Dev. Technol. 20, 12–21. https://doi.org/10.3109/10837450.2014.954728.

Mangal, H., Kirsolak, M., Kleinebudde, P., 2016. Roll compaction/dry granulation: suitability of different binders. Int. J. Pharm. 503, 213–219. https://doi.org/10.1016/j.ijpharm.2016.03.015.

Matić, J., Paudel, A., Bauer, H., Garcia, R.A.L., Biedrzycka, K., Khinast, J.G., 2020. Developing HME-based drug products using emerging science: a fast-track roadmap from concept to clinical batch. AAPS PharmSciTech 21, 1–18. https://doi.org/10.1208/s12249-020-01713-0.

Mendonsa, N., Almutairy, B., Kallakunta, V.R., Sarabu, S., Thipsay, P., Bandari, S., Repka, M.A., 2020. Manufacturing strategies to develop amorphous solid dispersions: an overview. J. Drug Deliv. Sci. Technol. https://doi.org/10.1016/j.jddst.2019.101459.

Mishra, S.M., Rohera, B.D., 2019. Mechanics of tablet formation: a comparative evaluation of percolation theory with classical concepts. Pharm. Dev. Technol. 24, 954–966. https://doi.org/10.1080/10837450.2019.1599913.

Mudie, D.M., Buchanan, S., Stewart, A.M., Smith, A., Shepard, K.B., Biswas, N., Marshall, D., Ekdahl, A., Pluntze, A., Craig, C.D., Morgen, M.M., Baumann, J.M., Vodak, D.T., 2020. A novel architecture for achieving high drug loading in amorphous spray dried dispersion tablets. Int. J. Pharm. X 2, 100042. https://doi.org/10.1016/j.ijpx.2020.100042.

Onuki, Y., Kosugi, A., Hamaguchi, M., Marumo, Y., Kumada, S., Hirai, D., Ikeda, J., Hayashi, Y., 2018. A comparative study of disintegration actions of various disintegrants using Kohonen's self-organizing maps. J. Drug Deliv. Sci. Technol. 43, 141–148. https://doi.org/10.1016/j.jddst.2017.10.002.

Pitt, K.G., Heasley, M.G., 2013. Determination of the tensile strength of elongated tablets. Powder Technol. 238, 169–175. https://doi.org/10.1016/j.powtec.2011.12.060.

Roberts, M., Ehtezazi, T., Compernolle, A., Amin, K., 2011. The effect of spray drying on the compaction properties of hypromellose acetate succinate. Drug Dev. Ind. Pharm. 37, 268–273. https://doi.org/10.3109/03639045.2010.509349.

Sandhu, H., Shah, N., Chokshi, H., Malick, A.W., 2014. Overview of amorphous solid dispersion technologies. In: Shah, N., Sandhu, H., Choi, D.S., Chokshi, H., Malick, A. W. (Eds.), Amorhous Solid Dispersion Theory and Practice. Springer, New York, pp. 91–122. https://doi.org/10.1007/978-1-4939-1598-9.

Sarabu, S., Kallakunta, V.R., Bandari, S., Batra, A., Bi, V., Durig, T., Zhang, F., Repka, M. A., 2020. Hypromellose acetate succinate based amorphous solid dispersions via hot melt extrusion: effect of drug physicochemical properties. Carbohydr. Polym. 233, 115828. https://doi.org/10.1016/j.carbpol.2020.115828.

Schittny, A., Huwyler, J., Puchkov, M., 2020. Mechanisms of increased bioavailability through amorphous solid dispersions: a review. Drug Deliv. 27, 110–127. https://doi.org/10.1080/10717544.2019.1704940.

Solanki, N.G., Gumaste, S.G., Shah, A.V., Serajuddin, A.T.M., 2019. Effects of surfactants on itraconazole-hydroxypropyl methylcellulose acetate succinate solid dispersion prepared by hot melt extrusion. II: Rheological analysis and extrudability testing. J. Pharm. Sci. 108, 3063–3073. https://doi.org/10.1016/j.xphs.2019.05.010.

Sun, C. Calvin, Himmelspach, M.W., 2006. Reduced tabletability of roller compacted granules as a result of granule size enlargement. J. Pharm. Sci. 95, 200–206. https://doi.org/10.1002/jps.20531.

Sun, C.C., Kleinebudde, P., 2016. Mini review: mechanisms to the loss of tabletability by dry granulation. Eur. J. Pharm. Biopharm. https://doi.org/10.1016/j.ejpb.2016.04.003.

Tanno, F., Nishiyama, Y., Kokubo, H., Obara, S., 2004. Evaluation of hypromellose acetate succinate (HPMCAS) as a carrier in solid dispersions. Drug Dev. Ind. Pharm. 30, 9–17. https://doi.org/10.1081/DDC-120027506.

Thompson, M.P., Pantin, W.C., Vernon, M., Charlton, S.T., Dennis, A.B., Timmins, P., 2010. Investigation of the effects of sodium lauryl sulphate on the roller compaction of spray dried dispersions. J. Pharm. Pharmacol. 62, 1447–1448.

Tye, C.K., Sun, C. Calvin, Amidon, G.E., 2005. Evaluation of the effects of tableting speed on the relationships between compaction pressure, tablet tensile strength, and tablet solid fraction. J. Pharm. Sci. 94, 465–472. https://doi.org/10.1002/jps.20262.

Yu, J., Xu, B., Zhang, K., Shi, C., Zhang, Z., Fu, J., Qiao, Y., 2019. Using a material library to understand the impacts of raw material properties on ribbon quality in roll compaction. Pharmaceutics 11. https://doi.org/10.3390/pharmaceutics11120662.

Zhang, D., Lee, Y.C., Shabani, Z., Lamm, C.F., Zhu, W., Li, Y., Templeton, A., 2018. Processing impact on performance of solid dispersions. Pharmaceutics 10. https://doi.org/10.3390/pharmaceutics10030142.

Zhao, N., Augsburger, L.L., 2006. The influence of product brand-to-brand variability on superdisintegrant performance: a case study with croscarmellose sodium. Pharm. Dev. Technol. 11, 179–185. https://doi.org/10.1080/10837450600561281.